2021 IEEE International Conference on Microwaves, Antennas, Communications and Electronic Systems (COMCAS) | 978-1-6654-3557-4/21/$31.00 ©2021 IEEE | DOI: 10.1109/COMCAS52219.2021.9628995

Intelligent Reflecting Surface Configuration Using Adaptive Quantization and Neural Prior

Tomer Fireaizen[1] Dan Ben-David[1] Shaked Hadad[1] Gal Metzer[2] Nir Kurland[1] Sima Etkind[1]
Pavel Lifshits[1] Yair Moshe[1] Israel Cohen[1]

[1]Signal and Image Processing Laboratory (SIPL), Faculty of Electrical and Computer Engineering
Technion – Israel Institute of Technology, Haifa, Israel, https://sipl.eelabs.technion.ac.il
[2]Faculty of Engineering, Tel Aviv University, Tel Aviv, Israel

***Abstract*—Intelligent Reflective Surface (IRS) is a promising technology for improving the data transmission rate in hard direct channel conditions. In this paper, we describe our solution to estimate the relevant channels and configure the IRS for efficient wireless communications, as part of the 2021 IEEE Signal Processing Cup (SP Cup) competition. First, we estimate the wireless channel and then find an IRS configuration that maximizes the rate of that channel. We begin with the provided far-from-optimal IRS configurations and apply an iterative optimization technique based on gradient descent and adaptive quantization. Further optimization is obtained by training a deep generative neural network to find a configuration that maximizes the rate function. Compared to the best provided configurations that provide a weighted average rate of 104.07 Mbit/s, the best configurations we discovered provide a significantly higher average rate of 120.70 Mbit/s. Non-IRS based solution provides an average rate of 4.38 Mbit/s.**

***Index Terms*—Channel estimation, IEEE Signal Processing Cup (SP Cup), Intelligent reflective surface (IRS), Neural prior, OFDM, Passive beamforming, Reconfigurable Intelligent Surface (RIS)**

I. Introduction

An Intelligent Reflecting Surface (IRS) [1] is a two-dimensional array of metamaterial whose interaction with electromagnetic waves can be controlled. It consists of an array of N discrete passive elements that can be controlled to alter the amplitude and/or phase of the reflected signal, thereby smartly reconfigure the wireless propagation environment. The physical implementation of such a system encounters many challenges. It is therefore important to design a generic algorithmic solution for utilizing IRS technology that is based on a small amount of prior knowledge on the properties the specific IRS, and employs as few stages as possible. Our goal is to characterize the behaviour of an IRS based on received signals from an over-the-air signalling, i.e., develop efficient channel estimation process and a control algorithm to configure the surface to increase communication performance [2].

The relation in the discrete-time domain between a transmitted signal $\boldsymbol{x}[\boldsymbol{k}]$ and the received signal $\boldsymbol{z}[\boldsymbol{k}]$ can be modeled as

$$z[k] = \sum_{\ell=0}^{M-1} h_{\boldsymbol{\theta}}[\ell] x[k-\ell] + w[k] \tag{1}$$

where $\{h_{\boldsymbol{\theta}} : \ell = 0 \dots M-1\}$ is the finite impulse response representation of the channel between the base station to the receiver, $\boldsymbol{\theta} \in \mathbb{R}^{1\times N}$ is the IRS specific configuration, and $\boldsymbol{w}$ is the receiver noise. The transmission over the communication channel is carried out using an orthogonal frequency-division multiplexing (OFDM) with a finite impulse response (FIR) filter of order M and $K > M$ subcarriers. A more detailed overview of fundamental properties of IRS technology from a signal processing perspective can be found in [3].

Evaluation in the SP Cup 2021 competition is based on an ensemble of 50 users that are located in the same room with the IRS. The transmitting base station and the IRS are at fixed locations and have a line-of-sight (LOS) channel between them. All users have non-line-of-sight (NLOS) channels to the base station. Some users have LOS channels from the IRS, as shown in Figure 1, others do not. The weighted average data rate over all users with the submitted configurations is computed according to [2] with double weight for NLOS users. The noise power spectral density is required to compute the rate, thus we should estimate the wireless channel for each user. An additional initial stage contains more data and is focused on a single user. Therefore, it can be utilized to learn channel-related and IRS-related channel properties, and to develop a technique for channel estimation. In Section II, we describe our technique for channel estimation. This technique uses the geometrical shape of the IRS that is found as described in Section IV.

Finding the global optimal configuration is mathematically intractable. With the growing interest in this technology, many heuristic solutions have recently been proposed. One notable solution is based on strongest tap maximization (STM) [4], [5]. However, this solution is inapplicable in practice as it assumes a continuous phase, whereas we are constrained to only two phases with a phase-shift difference of approximately π between the elements. Other methods were proposed to the discrete phase case, but they assume perfect knowledge of the channel state information (CSI) [6], [7] and prior knowledge of the geometrical shape and physical implementation of the IRS [5], [8], while we do not assume either one of them. The problem with these assumptions are that the IRS is a

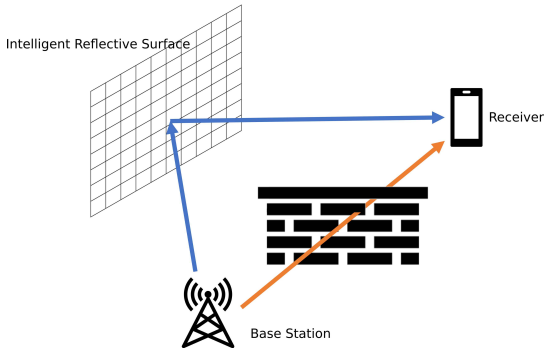

Fig. 1. Wireless communication with IRS: The base station has no LOS to the receiver, but it does has LOS to the IRS, which it uses to improve the data transmission rate.

passive device and therefore does not contain any active radio frequency (RF) chains. Thus, it is impossible to find out directly the channel from the base station to the IRS and from the IRS to the receiver, but only the cascaded channel from the base station through the IRS and to the receiver, using pilot signals sent from the base station to the receiver.

Let

$$\boldsymbol{z}^f = \boldsymbol{h}_{\boldsymbol{\theta}}^f \boldsymbol{x}^f + \boldsymbol{w} \tag{2}$$

be the received pilot signals in the frequency domain, where

$$\boldsymbol{h}_{\boldsymbol{\theta}}^f = \boldsymbol{h}_d^f + \boldsymbol{V}_a^f \boldsymbol{\theta} \boldsymbol{V}_b^f, \tag{3}$$

$\boldsymbol{h}_d^f \in \mathbb{C}^{K\times 1}$ is the uncontrollable paths channel, $\boldsymbol{V}_a^f, \boldsymbol{V}_b^f \in \mathbb{C}^{K\times N}$ are the channels from the base station to the N IRS elements and from them to the receiver, respectively, and $\boldsymbol{\theta} \in \mathbb{C}^{N\times N}$ is a diagonal matrix whose main diagonal contains the phases of the IRS elements. One can see that any attempt to estimate directly $\boldsymbol{V}_a^f$ or $\boldsymbol{V}_b^f$ is practically impossible, as they are invariant to multiplication by any diagonal matrix $\boldsymbol{A} \in \mathbb{C}^{N\times N}$ since:

$$\begin{aligned} \boldsymbol{z}^f &= (\boldsymbol{h}_d^f + \boldsymbol{V}_a^f \boldsymbol{\theta} \boldsymbol{V}_b^f)\boldsymbol{x}^f + \boldsymbol{w} \\ &= (\boldsymbol{h}_d^f + \boldsymbol{V}_a^f \boldsymbol{A}\boldsymbol{\theta}\boldsymbol{A}^{-1} \boldsymbol{V}_b^f)\boldsymbol{x}^f + \boldsymbol{w}\,. \end{aligned} \tag{4}$$

In the SP Cup 2021 we received two datasets: The first contains 4×4096 over-the-air signals received by one user equipment; each corresponds to a single IRS configuration. The second dataset contains 50×4096 over-the-air signals, 4096 signals for each of the 50 users, corresponding to a fixed subset of the IRS configurations from the first dataset. The IRS has $N = 4096$ elements but the geometrical shape of the IRS, as well as the locations of the base station, the IRS and the users, are unknown.

We present two novel algorithms for IRS configuration optimization. The first algorithm combines an adaptive quantization method with incremental optimization for quantization of the STM algorithm for continuous phase [4], [5]. Our second algorithm is based on the pioneering work of Deep Image Prior [9] that introduced the use of a *neural prior* in the context of image reconstruction, as well as [10]–[12] that extended the neural prior to other problems and representations such as 3D meshes, point clouds, and denoising. We have observed that arbitrary phase changes tend to reduce data transmission rates, while outputs subjected to a neural prior perform better. This observation is supported by [13], [14], which claims that IRS configuration should contain strong self-similarity. Moreover, it was shown in [15] that the over parameterization, which is inherently available in neural networks, helps in overcoming local minimums in optimization schemes like gradient decent, even for simple tasks such as linear kernel estimation. The design of our second algorithm is inspired by these previous works, exploiting the neural prior and the over parameterization that networks offer, to find a better global configuration that maximizes the rate. Our solutions for finding a good IRS configuration under these constraints is described in Section III.

II. Channel Estimation

Accurate channel estimation is critical for finding a good configuration because estimating the channel inaccurately may result in optimizing the wrong objective function. We model the system by

$$\boldsymbol{z} = (\boldsymbol{h}_d + \boldsymbol{V}\boldsymbol{\theta}) \odot \boldsymbol{x} + \boldsymbol{w}, \tag{5}$$

where $\boldsymbol{x}$, $\boldsymbol{z}$, $\boldsymbol{h}_d$ and $\boldsymbol{w}$ are vectors of size $K \times 1$ representing the transmitted signal, the received signal, the direct channel and the noise, respectively. $\boldsymbol{V}$ is a $K \times N$ matrix representing the cascade of the channel from the transmitter to the IRS and the channel from the IRS to the receiver, and $\boldsymbol{\theta}$ is a vector of size $N \times 1$ representing the configuration of the IRS. $\odot$ denotes the Hadamard element-wise product.

During the pilot transmission, all elements of $\boldsymbol{x}$ are equal to a scalar value $x_i \equiv \alpha$. The IRS is configured in a sequence of N configurations $\boldsymbol{\theta}_1, \ldots, \boldsymbol{\theta}_N$ that form the columns of an $N \times N$ Hadamard matrix H_N [16]. The first stage of channel estimation consists of a set of $4N$ configurations such that each configuration from H_N and its negation appear twice in the $N \times 4N$ configuration matrix of this sequence. Thus, summation over all received signals in this sequence yields $4N\boldsymbol{h}_d \odot \boldsymbol{x} + \sum_{i=1}^{4N} \boldsymbol{w}_i$, and we can find the direct channel by dividing this expression by $4N\alpha$. Summing over all N received signals of a single user in H_N we get $(N\boldsymbol{h}_d + \boldsymbol{V}\sum_{i=1}^{N}\boldsymbol{\theta}_i) \odot x + \sum_{i=1}^{N}\boldsymbol{w}_i$, where $\sum_{i=1}^{N}\boldsymbol{\theta}_i = [N, 0, .., 0]^T$ is a vector of size N. This expression gives us the sum of the direct channel and the response of the first element of the IRS to the +1 state. Since the first element is negligible, we estimate the direct channel of a single user in by

$$\begin{aligned} \hat{\boldsymbol{h}}_d &= \frac{\sum_{i=1}^{N}\boldsymbol{z}_i}{N\alpha} \\ &= \boldsymbol{h}_d + \boldsymbol{V}\cdot[1, 0, .., 0]^T + \frac{\sum_{i=1}^{N}\boldsymbol{w}_i}{N\alpha}\,. \end{aligned} \tag{6}$$

After estimating the direct channel $\boldsymbol{h}_d$ we can estimate the non-direct channel $\boldsymbol{V}$. Since the Hadamard matrix is invertible, we can use the least-square (LS) estimator that is given by

$$\boldsymbol{V} = (\boldsymbol{Z} - \boldsymbol{X}\ \boldsymbol{H}_d)\,\boldsymbol{\Omega}^{-1}/\alpha, \tag{7}$$

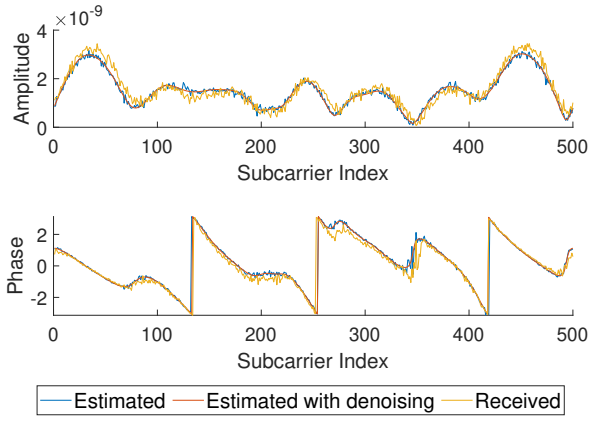

Fig. 2. Verification of our channel estimation process from N configurations, with and without denoising, with the $4N$ configurations of the first pilot stage.

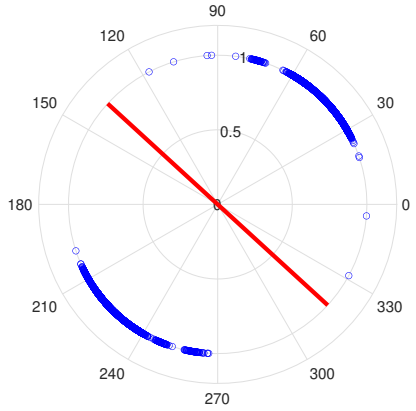

Fig. 3. An example of phase quantization for the resulting STM configuration for user 20. The best separating line is drawn in red.

where $\boldsymbol{X} = \alpha I_{K\times K}$ is a $K \times K$ matrix of the transmitted signal (the scalar α), $\boldsymbol{Z}$ is a $K \times N$ matrix whose columns are the received signals, $\boldsymbol{H}_d$ is a $K \times N$ matrix whose columns are the direct channels $\boldsymbol{h}_d$, and $\boldsymbol{\Omega}$ is the Hadamard matrix.

We used our discovery of the array's geometrical shape (described in Section IV) to compensate the estimated channel for the addition of the response of the first element of the IRS to the +1 state. We assume, and verified this on the set of pilot signals from the first stage, that the MSE between the frequency response of each element i and the frequency response of elements $i + 64n$ (elements in the same column) is small. So, we take the first column of $\boldsymbol{V}$ to be

$$\boldsymbol{V}(:,1) = \frac{1}{63}\sum_{n=1}^{63} \boldsymbol{V}(:, 1 + 64 \cdot n)\,. \tag{8}$$

We also perform a similar compensation for the direct channel $\boldsymbol{h}_d$.

LS-based channel estimation is simple to implement and does not require any a-priori knowledge of channel statistics. However, its performance is not as good as more advanced channel estimation techniques. Therefore, we applied a denoising strategy inspired by [17]. The channel in the time domain is a vector of size K with small non-zero values at its $[M+1, .., K]$ elements. Since the channel in the time domain is modeled as an FIR filter of order M, we assume that the elements $[M + 1, .., K]$ in the channel vector are noise, and set them to zero before returning to the frequency domain. The estimator we get from this process yields zero MSE on the N configurations of H_N. When verified on data from the first stage, this estimator results in the smallest MSE of any other channel estimation methods we tried. Figure 2 shows the verification of our channel estimation process on the first stage. Both channel estimators from N configurations follow closely the amplitude and phase of the channel computed from $4N$ configurations. The channel estimated after denoising is smoother.

III. Configuration Search

To find a configuration that maximizes the data rate, we use two techniques. The first is an adaptive quantization and optimization, while the second uses a deep neural network as a prior for the configuration search.

Adaptive Quantization. In the first technique, we try to maximize the rate $\mathcal{R}$ (calculated according to [2]) using the gradient descent algorithm by defining $\nabla_{\vec{\theta}}\mathcal{R} = \frac{\partial \mathcal{R}}{\partial \vec{\theta}}$ and an update rule

$$\vec{\theta}^{t+1} = \exp\left[\angle\theta^t + \frac{\angle\nabla_{\vec{\theta}}\mathcal{R}}{\left\|\nabla_{\vec{\theta}}\mathcal{R}\right\|}\right] \tag{9}$$

where $\angle\theta$ is the phase of the complex vector $\theta \in \mathbb{C}^{4096}$. After several iterations, the optimization converges to a local maximum that serves as the initial value for an iterative optimization and quantization algorithm. We quantize the phase into two values by finding the best line for separating the phases on the unit circle for each user. An example of such separating line for phase quantization is depicted in Figure 3. Let the best separating line be $[\tilde{\phi}, \tilde{\phi}+\pi]$. Then, for all element phases calculated using the STM estimator, we calculate their cyclic distance from the separating line: $\mathcal{D} \equiv \sin^2(\angle\theta - \tilde{\phi})$. This metric assigns a lower distance to elements that have more ambiguous clustering. The iterative process is described in Algorithm 1. More ambiguous elements are assigned a lower distance based on the assumption that they are more likely to be quantized incorrectly, and have a better chance of increasing the rate. Therefore, as the algorithm proceeds, it is more likely to converge to the optimal IRS configuration, as the optimal elements to be considered are re-evaluated more frequently.

To prevent the above algorithm from entering a local maximum, at each 4^n step of the algorithm, where $n \in \{1, 2, ... \log_4(4096)\}$, we check each element to see if its phase change yields a higher rate. Another means for preventing entry to a local maximum is to use a probabilistic method at the end of the algorithm. Each element is assigned a probability that is inversely proportional to the distance

Algorithm 1: Iterative Optimization and Quantization

Result: IRS configuration
repeat
  Calculate $\mathcal{D}(\angle\theta)$
  $e = \text{argmin}(\mathcal{D}(\angle\theta))$
  Create two assumptions - e is either $+1$ or -1.
  For each assumption, run gradient descent optimization for all unfixed elements until convergence.
  Fix e to the value that yields higher data rate.
until *All IRS elements are fixed*;

from its phase value assigned by the continuous phase STM estimator. We then select a random configuration based on these probabilities. If the new configuration has a higher rate than the original, the new configuration is set as the base configuration for an additional random iteration (with the original probabilities). This process is repeated a fixed number of iterations.

Neural Optimization. The second technique we use for configuration search, generates IRS configurations by maximizing the rate while using a randomly initialized neural network as a regularization term for the optimization process, *i.e.*, applies a *neural prior*. [13], [14] proposed that a favorable solution for the phase configuration should contain strong self-similarity, supporting the use of a neural prior for IRS configuration search. Furthermore, [15] showed that using over parameterization, which is inherently available in neural networks, is beneficial in avoiding local minima during the optimization process, and to reach a better final solution, even for simple problems such as linear kernel estimation. Consequently, we hypothesize that a *neural prior* may also be favorable for solving the IRS configuration problem, as it is subject to a neural network that produces self-similar results, and is able to avoid local optimization minimums better than direct optimization.

We define our loss function to be minus the data transmission rate, and optimize a network to overfit a phase configuration for one specific user. We observe that LOS users achieve high data rates with very smooth, columns-like, configurations. We conclude that the steering components of the configurations are highly important, especially for LOS users. Therefore, we divide the configuration search architecture into two sub-networks, as shown in Figures 4 and 5. The first sub-network receives a random scalar as input, similar to [9], [10], and optimizes for the steering configuration (according to the geometrical shape of the array, see Section IV), while the second sub-network receives this steering configuration as input and generates another, not necessarily steering, final configuration. The purpose of the second sub-network is to fine tune the steering configuration by adding elevation components. The first sub-network consists of five fully-connected layers interspersed by one hyperbolic tangent activation function, and a final hyperbolic tangent activation on

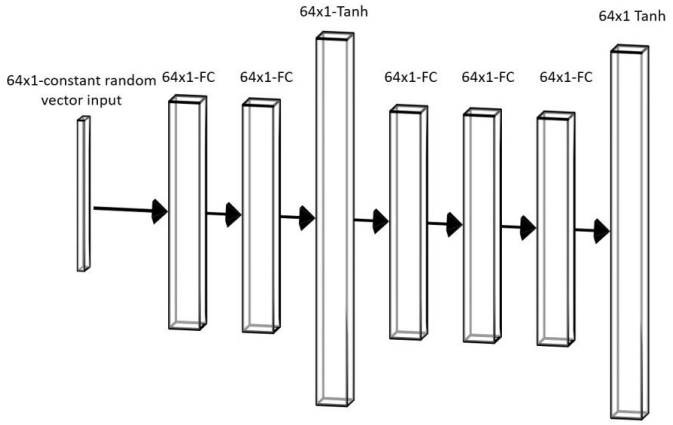

Fig. 4. First sub-network of the proposed generative neural network architecture. This network receives a random scalar (in vector form) as input and generates a steering configuration (in vector form).

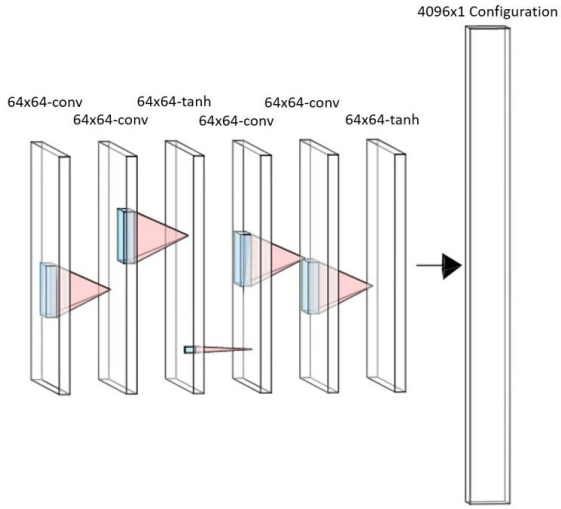

Fig. 5. Second sub-network of the proposed generative neural network architecture. This network receives a steering configuration as input and generates another, not necessarily steering, configuration (in vector form).

the output vector. The use of multiple consecutive linear layers is not equivalent to having a single larger fully-connected layer for optimization purposes, as was shown in [15]. In fact, this creates the desired over parameterization, by decomposing a single equivalent linear layer into multiple linear layers, which helps to avoid local minimas throughout the optimization process. The resulting vector of size 64×1 represents the columns of a steering configuration and is replicated to create a 64×64 matrix that is the input to the second sub-network. The second sub-network is a fully convolutional neural network with intermediate layers of hyperbolic tangent activation function that generates the final configuration as vector of size 4096×1. The choice of the fully convolutional architecture for the second part is motivated by our assumption that elevation components should not have long range dependency, but rather be affected by local changes.

For optimizing the sub-networks, we used gradient de-

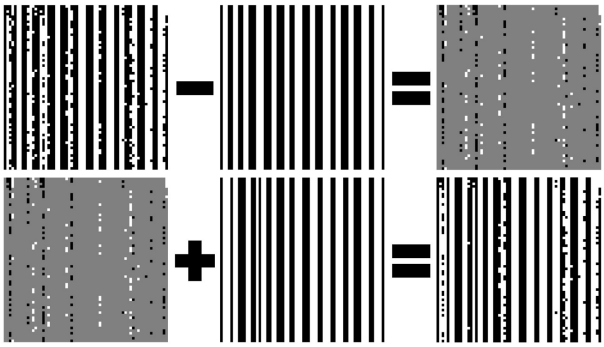

Fig. 6. Combination of our two configuration search techniques - we extract the elevation component from the best configuration discovered by the first technique, and re-estimate the steering component using the first generative sub-network from our second technique. Then, we sum the two components to obtain the final configuration.

TABLE I
MEAN DATA RATES FOR THE IEEE SP CUP 2021 WITH NO IRS AND FOR THE THREE PROPOSED IRS CONFIGURATION TECHNIQUES. THE GENERATIVE NETWORK YIELDS THE HIGHEST RATE FOR LOS USERS, BUT WITH INFERIOR PERFORMANCES FOR NLOS USERS.

Algorithm	LOS	NLOS
No IRS	3.95 $\frac{Mbits}{sec}$	3.62 $\frac{Mbits}{sec}$
Adaptive Quantization	116.88 $\frac{Mbits}{sec}$	65.17 $\frac{Mbits}{sec}$
Neural Prior	**117.09** $\frac{Mbits}{sec}$	65.06 $\frac{Mbits}{sec}$
Steering-Elevation Decomposition	-	**65.25** $\frac{Mbits}{sec}$

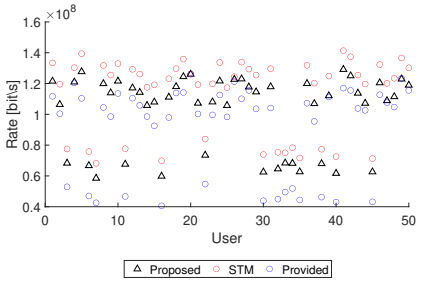

Fig. 7. Data rates obtained for each user with the best IRS configuration in our proposed solution compared to the data rates obtained by the best configuration provided in the pilot stage and to the data rate obtained by STM (with continuous phase). The 36 users at the top of the graph have LOS with the IRS, while the other 14 users at the bottom do not.

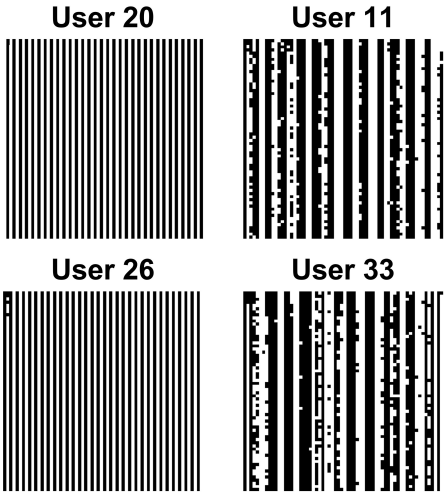

Fig. 8. An example of the best configurations discovered by our proposed solution. Both users on the left have LOS with the IRS so their best configuration is almost pure steering. Both users on the right do not have LOS with the IRS so the patterns in their best configuration are more intricate.

cent with cosine annealing learning, compared to our first configuration search technique which used vanilla gradient descent and adaptive quantization. The network optimization solution converges faster, is computationally more efficient and typically discovers configurations with higher data rates for LOS users. However, for NLOS users, the first technique is usually better, as these users require a stronger emphasis on elevating phase components.

In an effort to combine the best of both solutions, we combined our two configuration search techniques by decomposing the configuration into its steering and elevation basis, as depicted in Figure 6. We extracted the elevation component from the best configuration discovered by the first adaptive quantization technique, and estimated an independent steering component using the first generative sub-network from our second technique. Then, we summed the two components to obtain the final configuration. This technique improved on average the data transmission rates for the NLOS users, compared to using each technique separately. The results of these three method are compared in Table I. A weighted average rate over all users that doubles the rate for NLOS users is calculated according to [2]. Compared to the best configurations provided to all users that provide an average rate of 104.07 Mbit/s, the best configurations we discovered provide a significantly higher average rate of 120.70 Mbit/s. Without IRS, the average rate is only 4.38 Mbit/s.

Figure 7 shows the data rate for each user with the best IRS configuration we found compared to the data rate obtained by the best configuration provided in the pilot stage and to the data rate obtained by STM (with continuous phase). Users at the top of the graph have LOS with the IRS, while users at the bottom do not. Figure 8 shows examples of the best configurations discovered by our proposed solution. Users in LOS with the IRS have best configurations that are almost pure steering, while users with no LOS with the IRS have more intricate patterns in their best configurations.

IV. GEOMETRICAL SHAPE OF THE IRS

Knowing the geometrical shape of the IRS allows to utilize the spatial correlation between elements as described in Sec-

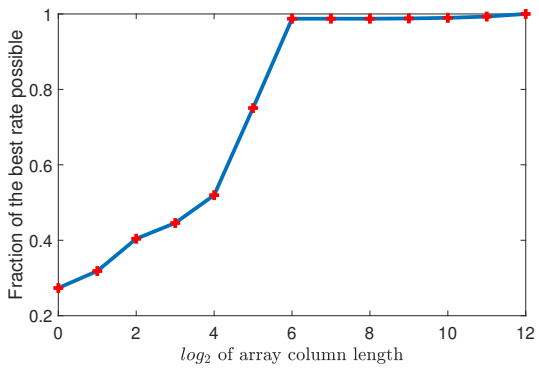

Fig. 9. Average data rate for all LOS users as a function of the IRS array column length. The best possible rate begins with $log_2 n = 6$, so we can conclude that the physical shape of the array is 64×64 elements.

tion III. In the SP Cup 2021 competition, the IRS is rectangular and has $N = 4096$ elements. Hence, it can have one of the sizes $1 \times 4096, 2 \times 2048, ..., 4096 \times 1$. We assume that for users in LOS with the IRS, a pure steering configuration will provide a high data rate. We observe that these steering configurations for LOS users have many columns of the same value along the y-axis. Thus, we have implemented a version of STM that allows only steering configurations. We then used this version to find the best steering configuration for all LOS users for each possible geometrical shape of the array, and compared the rates obtained by the different geometrical shapes. The results of this experiment are depicted in Figure 9. From this figure we can conclude that the physical shape of the IRS is 64×64 elements.

V. Conclusions

In this paper, we approach the IRS configuration optimization problem from two different perspectives: adaptive quantization and optimization, and a novel *neural prior* approach. We have shown that the recently proposed ideas of *neural prior* and over-parametrization in generative neural networks can be extended to the world of RF communications, far from their original use in computer vision. This approach achieves high data transmission rates for LOS users but is less effective for NLOS users. We obtain high data transmission rates for all users by combining the two proposed configuration search techniques.

We demonstrated that even with the IRS technology provided in the SP Cup 2021 competition, which uses only two phase states and has no control over the magnitude of the reflected signal, data transmission rate can be increased on average by a factor of 18 for NLOS user and by a factor of 30 for LOS user when compared to the non-IRS case. In addition, we have developed a technique for discovering the physical shape of the IRS array, and used an understanding of the physical properties of the IRS to improve the common linear channel estimation method. All of these techniques have allowed us to efficiently utilize IRS technology to significantly improve data transmission rates between the base station and users. The code of our solution is available at https://github.com/BIueMan/IEEE_SP_CUP_2021-SIPL_TEAM

VI. Acknowledgment

The authors would like to thank Prof. David Malah and Nimrod Peleg from the Signal and Image Processing Lab (SIPL) at the Technion for their continuous assistance and support.

References

[1] M. Di Renzo, A. Zappone, M. Debbah, M.-S. Alouini, C. Yuen, J. de Rosny, and S. Tretyakov, "Smart radio environments empowered by reconfigurable intelligent surfaces: How it works, state of research, and road ahead," *IEEE J. Sel. Areas Commun.*, vol. 38, no. 11, pp. 2450–2525, 2020.

[2] E. Björnson, "IEEE Signal Processing Cup 2021 - Configuring an Intelligent Reflecting Surface for wireless communications," 2021. [Online]. Available: https://github.com/emilbjornson/SP_Cup_2021

[3] E. Björnson, H. Wymeersch, B. Matthiesen, P. Popovski, L. Sanguinetti, and E. de Carvalho, "Reconfigurable intelligent surfaces: A signal processing perspective with wireless applications," *arXiv preprint arXiv:2102.00742*, 2021.

[4] B. Zheng and R. Zhang, "Intelligent reflecting surface-enhanced OFDM: Channel estimation and reflection optimization," *IEEE Wireless Communications Letters*, vol. 9, no. 4, pp. 518–522, 2019.

[5] S. Lin, B. Zheng, G. C. Alexandropoulos, M. Wen, F. Chen *et al.*, "Adaptive transmission for reconfigurable intelligent surface-assisted OFDM wireless communications," *IEEE Journal on Selected Areas in Communications*, vol. 38, no. 11, pp. 2653–2665, 2020.

[6] Q. Wu and R. Zhang, "Intelligent reflecting surface enhanced wireless network via joint active and passive beamforming," *IEEE Transactions on Wireless Communications*, vol. 18, no. 11, pp. 5394–5409, 2019.

[7] C. Huang, A. Zappone, G. C. Alexandropoulos, M. Debbah, and C. Yuen, "Reconfigurable intelligent surfaces for energy efficiency in wireless communication," *IEEE Transactions on Wireless Communications*, vol. 18, no. 8, pp. 4157–4170, 2019.

[8] B. Z. Changsheng You and R. Zhang, "Channel estimation and passive beamforming for intelligent reflecting surface: Discrete phase shift and progressive refinement," *IEEE Journal on Selected Areas in Communications*, vol. 38, no. 11, pp. 2604–2620, 2020.

[9] D. Ulyanov, A. Vedaldi, and V. Lempitsky, "Deep image prior," in *Proceedings of the IEEE conference on computer vision and pattern recognition*, 2018, pp. 9446–9454.

[10] R. Hanocka, G. Metzer, R. Giryes, and D. Cohen-Or, "Point2mesh: A self-prior for deformable meshes," *ACM Trans. Graph.*, vol. 39, no. 4, 2020.

[11] G. Metzer, R. Hanocka, R. Giryes, and D. Cohen-Or, "Self-sampling for neural point cloud consolidation," *arXiv preprint arXiv:2008.06471*, 2020.

[12] F. Hashimoto, H. Ohba, K. Ote, A. Kakimoto, H. Tsukada, and Y. Ouchi, "4d deep image prior: dynamic pet image denoising using an unsupervised four-dimensional branch convolutional neural network," *Physics in Medicine & Biology*, vol. 66, no. 1, p. 015006, 2021.

[13] C. You, B. Zheng, and R. Zhang, "Progressive channel estimation and passive beamforming for intelligent reflecting surface with discrete phase shifts," 2019. [Online]. Available: http://arxiv.org/abs/1912.10646

[14] E. Björnson, "Optimizing a binary intelligent reflecting surface for OFDM communications under mutual coupling," *CoRR*, vol. abs/2106.04280, 2021. [Online]. Available: https://arxiv.org/abs/2106.04280

[15] S. Bell-Kligler, A. Shocher, and M. Irani, "Blind super-resolution kernel estimation using an internal-gan," *arXiv preprint arXiv:1909.06581*, 2019.

[16] B. Z. Changsheng You and R. Zhang, "Channel estimation and passive beamforming for intelligent reflecting surface: Discrete phase shift and progressive refinement," *arXiv preprint arXiv:1912.10646v2*, 2020.

[17] P. Sure and C. M. Bhuma, "A survey on OFDM channel estimation techniques based on denoising strategies," *Engineering Science and Technology, an International Journal*, vol. 20, no. 2, pp. 629–636, 2017.